A comparative assessment of satellite-derived Adriatic Sea surface temperature

I. TOMAŽIĆ*†, M. KUZMIĆ†, G. NOTARSTEFANO‡, E. MAURI‡ and P.M. POULAIN‡

†Center for Marine and Environmental Research, Ruđer Bošković Institute, Zagreb, Croatia
‡Istituto Nazionale di Oceanografia e di Geofisca Sperimentale, Trieste, Italy

Abstract

In this paper, five AVHRR- and four MODIS-based Adriatic-focused satellite SST products are analysed and compared with two sets of in situ SST measurements: a drifter-based dataset collected in 2003, and a platform-based dataset gathered in 2004; an additional set was used to validate the new SST coefficients. Analysis of satellite minus in situ SST residuals shows similar results for both in situ datasets, with the differences being within 0.2 K. All daytime SST biases exhibited positive values (less than 0.5 K). Nighttime biases for short-wave IR algorithms exhibited near zero and small negative values with an exceptionally low standard deviation (about 0.3 K) regardless of the sensor used. Analysis of filtered residual time-series allowed direct comparison between different SST products. The seasonal change in the daytime biases was found to covary with similar changes in atmospheric water vapour and the Adriatic specific wind regime.

Keywords: SST; Adriatic; AVHRR; MODIS; drifters; validation

1 Introduction

Sea surface temperature is among the most important geophysical parameters used in oceanography, meteorology and climatology; it is a key variable at the ocean-atmosphere boundary. In an era of global forecasting of ocean dynamics, there is an ever-increasing emphasis on error assessment of this parameter (Donlon et al, 2007). Satellite SST (for all acronyms see Appendix) measurements allow simultaneously high spatio-temporal resolution and global coverage, unmatched by in situ measurements. However, the empirical nature of the coefficients in SST algorithms entails their calibration and validation with in situ measurements. Although global SST fields often exhibit a near-zero bias, appreciable differences may appear on regional scales, suggesting geographical and seasonal biases. Zhang et al (2004) found global averages rarely exceed 0.2 °C because of regional biases with opposite signs cancelling each other out. Acknowledging that these biases can locally exceed 0.5 °C and exhibit a seasonal relation to atmospheric conditions, the authors suggested that satellite SST retrieval algorithms should be

space and time dependent. Kumar et al (2000) investigated the performance of the global Pathfinder algorithm in several regional conditions. They found the best discrepancy that could be expected between satellite and buoy data to be ~0.5 K, with the satellite underestimating SST in most of the studied regions. Seasonal modulation of the differences between satellite and in situ SST was observed in many world-ocean regions with the residuals further exhibiting inter-annual variation. Validation of Pathfinder satellite data in the Mediterranean Sea with CTD and XBT in situ SST data revealed a bias of -0.2 K (D'Ortenzio et al, 2000), whereas validation of its accuracy with a limited set of M-AERI measured skin SST data exhibited a bias of 0.07 K and an exceptionally low SD of 0.31 K (Kearns et al, 2000). Arbelo et al (2000) demonstrated an inadequate performance of the operational SST split-window algorithm in a subtropical region. Their locally derived set of SST coefficients outperformed the global counterpart whenever local atmospheric conditions differed from the first guess atmospheric state. Minnett et al (2004) showed an improvement in MODIS-based SST retrieval with an SD in the range between 0.4 K and 0.5 K and a small negative bias on a global scale. Direct comparison between coincident observations of Terra/MODIS and NOAA16/AVHRR BTs (Cao and Heidneger, 2002) exhibited strong agreement within 0.3 K for both 11 μm and 12 μm bands. This difference vanished on average after applying SST retrieval coefficients for each sensor.

Generally, biases in satellite SST retrievals combine two forms of systematic error: prior error due to the implicit state of the atmosphere (for which regression coefficients are derived), and an error coming from the non-linearities in the SST-atmospheric state relation (Merchant et al, 2006). Both of these errors exhibit spatial and temporal variability and arise as a consequence of the retrieval form, rather than an inadequate set of retrieval coefficients (Merchant et al, 2006). To eliminate regional biases on the global scale, Merchant et al (2008) used the OE technique, where NWP forecast fields were used as prior information of the atmosphere and ocean expected state to derive simulated BT prior observations. Using three months of Metop-A data for comparison, they showed that OE application reduces regional biases (an absolute bias less than 0.1 K in 64% of 10°-latitude by 30°-longitude cells compared to only 33% of cells in the case of the NLSST algorithm). The SD is also reduced from 0.83 K to 0.42 K. Another approach to reduce regional and inter-sensor biases is to create multidimensional lookup tables using parameters like satellite zenith angles, BT differences, SST, wind speed and water vapour content (Castro et al, 2008). The NOAA normally validates their SST products on a monthly basis, but global matchups are sparse, geographically biased and take time to accumulate; Dash et al (2007) used SST climatology as a reference state to

*Corresponding author. Email: igor.tomazic@irb.hr

perform statistical analysis of anomalies and produce long-term quality control and assurance. The globally initiated GHRSST-PP project (Donlon et al, 2007) aims to resolve the regional and inter-sensor discrepancy issues by providing consistent, error-bounded products that combine several satellite-sensor and in situ SST datasets, explicitly taking care of individual SSES. In validation studies focused on the Adriatic Sea, the NOAA/AVHRR SST bias exhibited values between -0.3 and 0.5 K (Notarstefano et al, 2006, Tomazic et al, 2006), depending on the sensor, algorithm and analysed year.

Bearing in mind GHRSST-PP project standards and expectations, we performed a detailed, comparative, Adriatic-centred study of the Adriatic remotely-sensed SST. In performing the study, we aimed at elucidating cross-platform and inter- and intra- algorithm differences helping produce a consolidated Adriatic satellite SST product of the highest resolution and quality. To that end, we made use of several satellite SST products (AVHRR, MODIS, Pathfinder) and several in situ datasets (drifter SST, platform SST, shipboard SST). Lacking the foundation temperature measurements (free of diurnal variability), we calculated relative residual differences between the satellite and bulk in situ measurements. Early results along these lines are reported in Tomazic et al (2007). The rest of the paper is organised as follows: satellite, in situ and ancillary data used in the study are presented in the Data and algorithms section; the employed methods are presented in the third section and obtained results are discussed in the fourth section; the findings are summarised in the last section.

2 Data and algorithms

The data used in this study are divided into three groups; the first group comprises satellite measurements (nine satellite products); the second covers in situ SST measurements (three datasets collected with drifter-based, platform-based and ship-borne instruments); and the last makes up the ancillary data.

2.1 Satellite SST products

Of the nine satellite-derived SST products, the first four (based on AVHRR NOAA16/NOAA17 data) were produced locally, whereas the other five (based on MODIS-Aqua, MODIS-Terra data and Pathfinder processing) were devised elsewhere (Feldman and McClain, 2007; Casey, 2007).

Local AVHRR products are based on data acquired with the Quorum HRPT receiving station (nominal resolution of 1.1 km). The AVHRR data within the HRPT stream were processed to L1B level by the AAPP application supplied by EUMETSAT (NWP SAF) (Atkinson and Dohery, 2005) and additional navigational correction was performed with the ANA-3 application supplied by

METEO FRANCE, CMS (Brunel and Marsouin, 2002). Further processing to L2 level in the satellite projection was done with an 'in-house' application. The processing includes digital counts calibration to reflectance and BTs (Goodrum et al, 2000), interpolation/extrapolation of geolocation data to every pixel, landmasking, cloudmasking and deriving SST values from IR channels. The cloudmask scheme uses spectral and textural image features based on the thresholding scheme of Saunders and Kriebel (1988) and Stowe et al (1999) with the static thresholds tuned for the Adriatic Sea region (details in Tomazic, 2006). During the 2003-2004 period, 2568 NOAA16 and 2464 NOAA17 scenes were collected, with an average number of 6.9 scenes per day for both satellites. The SST derivation was based on NOAA/NESDIS operational SST algorithms, the NLSST for daytime and nighttime and MCTriple ('Andy') for nighttime only (Table 1).

The fifth AVHRR product is the 4 km Pathfinder SST version 5.0 developed at the University of Miami's RSMAS and retrieved from the PO.DAAC. For the years 2003 and 2004, the Pathfinder program used NOAA17 data, producing two fields per day (daytime and nighttime, altogether 1460 scenes). The Pathfinder product pixel registration exact time is partially known, introducing some ambiguity into the validation procedure (Casey, 2007). The problem lies in the processing procedure, which in the case of overlapping orbits uses multiple observations to create a single daytime or nighttime SST field. The approximate time of the Pathfinder pixels was found by analysing NOAA17 data from the local HRPT receiving station based on the assumption that if there are two clear pixels (maximum for the Adriatic) from two consecutive orbits for the same location, the pixel with the smaller satellite zenith angle is used in the Pathfinder dataset. The Pathfinder algorithm (Table 1) is based on the NLSST algorithm with a monthly variable set of coefficients for two different atmospheric regimes derived from regression with in situ buoy data (Kilpatrick et al, 2001). Later in the paper, we refer to this type of coefficient as 'variable', as opposed to a fixed set used in local AVHRR products. At the time of this study, there were no 'true' Pathfinder coefficients for the year 2004. Consequently, the interim version of the product was used.

The SST data derived from the MODIS sensor (for both Aqua and Terra platforms) were retrieved for the years 2003 and 2004 from the OBPG site (Feldman and McClain, 2007) as 5-minute granules in L2 format (V5.3 and V5.6 processing respectively) with a nominal resolution of 1 km. Two MODIS SST products for each satellite platform were used: the SST derived with the LWIR algorithm (MODSST) available for both daytime and nighttime passes, and the SST derived with the SWIR algorithm (MODSST4) available only for nighttime passes (Table 1 [Brown and Minnett, 1999]). Like Pathfinder, the MODSST/MODSST4 uses a variable set of coefficients, with the important difference of additionally adjustmenting the coefficients relative to the in situ skin

temperature measurements from the M-AERI radiometer (P.J. Minnett, personal communication). This correction produces skin SST for both MODSST and MODSST4 products. The other important difference (in this study) is the use of MODSST4 as the reference nighttime temperature in the MODSST algorithm (Table 1). Terra satellite Adriatic overpasses are 10:00 UTC (daytime) and 21:00 UTC (nighttime); the respective Aqua overpasses are 12:00 UTC and 01:00 UTC. Compared to the NOAA satellites, the Aqua overpass is closer to NOAA16, and the Terra to NOAA17. For the years 2003 and 2004, there were a total of 1790 Aqua and 1860 Terra granules for the Adriatic region, with an average number of 5.1 granules per day for both satellites.

2.2 In situ SST data

In situ data come from three sources with distinct space and time resolutions: drifter (a very high spatial and temporal resolution), platform (a single position but very high temporal resolution - 20 min) and shipborne (a low to medium resolution in both space and time). The third set was used only as an independent in situ reference.

Drifter-based data were collected during the DOLCEVITA project, (Ursella et al, 2004) spanning the time interval from 21 September 2002 to 29 February 2004. There were a total of 118 drifters and the majority were of the CODE type. On these drifters, the temperature sensor is positioned 40 cm below the surface and the accuracy is ±0.1 °C in a temperature range from -5 °C to 39 °C (Leitz, 1999). Geolocation accuracy is 200-300 metres for drifters equipped with the ARGOS system, and 10 metres for drifters equipped with the GPS system (Poulain et al, 2001). The wintertime cloud cover combined with uneven drifter temporal distribution led to the use of a quasi-continuous data period between 10 January 2003 and 17 September 2003, with a total number of 487001 SST measurements (on average 194 SST measurements per day). Their spatial distribution (Figure 1) shows very good coverage of the northern and middle Adriatic, while the southern part is poorly covered due to the initial release positions of the drifters (northern and middle Adriatic) and general cyclonic circulation.

Platform-based data come from the IVANA-A gas rig situated in the northern Adriatic [13° 17.9'E, 44° 44.7'N] (Figure 1) and cover the period from 2 February 2004 to 17 September 2004. The SST was measured with an Aanderaa TR7 thermistor chain (only 1 m depth data were used) with a 20-minute sampling interval. There were 15807 SST measurements in this period, with an average number of 69 measurements per day. Since there is no time overlap between the drifter and platform data, it was not possible to directly compare the two field measurement datasets.

Shipborne CTD measurements comprise the data taken as part of the ADRICOSM project (ADRICOSM) in 2003. The project combines data from 5 institutions covering 4 areas of the

Adriatic Sea (the Emilia Romagna area, Trieste Bay, the west Istrian coast, and the Split area). All measurements were made with CTD data instruments and a vertical resolution of 0.5 metres; a depth of 1 metre was used as the SST depth. Infrequent measurements led to a relatively small data set. On average, there are 20 data per day (when the measurements were performed), while in the summer months there are 50 data per day. It should be noted that this dataset contains only daytime measurements.

2.3 Ancillary data

Two different wind datasets and two different water vapour datasets were used to aid the analysis. The first wind dataset is the LAMI model output (7 km resolution, 10 metres height, every 3 hours), whereas the second comes from the QuikSCAT COGOW database (August 1999–July 2004, 10 m wind) (Risien and Chelton, 2006). LAMI data for the whole Adriatic were available for the year 2003; only the wind data closest to the IVANA-A platform were available for 2004. These wind data were interpolated to each matchup pair to assess their impact. In addition, LAMI and COGOW data were used in wind distribution calculation. Winds from the COGOW database were also used to compare the Adriatic wind regime with the open ocean one. The first tcwv dataset is derived from the MODIS data (Seemann et al, 2006) over the Adriatic Sea. Data were retrieved from NASA GSFC for the year 2003 and further averaged over the northern Adriatic Sea where the majority of matchups were located. The second tcwv dataset is an Adriatic subset of the ECMWF ERA-40 reanalysis data (Uppala et al, 2005). Monthly tcwv climatology is derived from the subset (Tomazic and Kuzmic, 2009.) for the 'wet' points over the Adriatic Sea, covering the period from September 1957 to August 2002.

3 Methods

Validation of the satellite SST products is based on the creation of an MDB of temporally and spatially coincident satellite and in situ SST measurements. The initial MDB is created requesting a maximum 1 hour of absolute time difference and a within-pixel spatial difference between the satellite overpass and in situ measurement. Whenever matchup criteria were satisfied, satellite data for the central satellite pixel and 9x9 surrounding pixels were extracted from the satellite image together with the corresponding in situ measurement (SST, position and date) and LAMI wind data, creating a matchup record. It should be noted that the vertical collocation of the satellite and in situ measurements is not the same for all satellite products. The AVHRR algorithms provide a bulk temperature suitable for comparison with in situ data, whereas MODIS-based algorithms estimate the skin temperature requiring a correction to the subskin temperature. The skin surface is on

average ~0.17 K cooler than the subskin layer (Donlon et al 2002) and therefore this difference is added to the MODIS SST to allow comparison. True comparison would include modelling diurnal stratification from the subskin to the corresponding in situ depth, but lacking the modelling information, we directly compared the $SST_{subskin}$ to the SST_{depth}, stressing the problems with such comparison.

In local processing of AVHRR data, besides the landmasking, cloudmasking and restriction on the satellite zenith angle below 50°, restricting criteria on channel 4 and 5 brightness temperatures were also applied (based on Eugenio et al, 2005) to eliminate possible errors in geolocation near SST fronts and errors in cloudmasking near cloud edges. In deriving channel 4 and 5 BTs, only central pixels with an SD less than 0.12 K (sensor NEΔT) of the corresponding surrounding 3x3 pixel window are included in the analysis. This criterion reduces the number of available matchup pairs by 15% but improves the quality of data. For MODIS and Pathfinder products, only SST values with the highest quality flags (values of 0 for MODIS and 7 for Pathfinder) were included in the analysis. The use of the highest quality flags ensured that only a couple of matchups have residuals larger than 3 K, and less than 1.5% have residuals larger than 2 K for all MDBs. An absolute temporal difference of 1 h could create matchups where the single satellite measurement is paired with multiple consecutive and similar in situ SST measurements, affecting the overall statistics. A unique one-to-one pairing was therefore imposed. Despite the 1h temporal difference, there were periods lacking any matchup pairs (pronounced cloudiness). For the drifter based MDBs, there were two such periods (end of January 2003 - beginning of February 2003, and in the middle of September 2003), whereas for the platform-based MDBs there were several smaller periods in the first half of the year 2004 (February, March, April).

4 Results and Analysis

The results are presented in two ways. Firstly, the overall statistics in the form of biases (means) and SDs of all residuals [satellite SST – in situ SST] in given time periods were calculated for the drifter and platform based MDBs; the respective periods are 10 January 2003 - 17 September 2003 and 2 February 2004 - 17 September 2004. These parameters, together with the number of matchup pairs, are presented for each MDB with respect to the satellite SST product, in situ database and time of day (daytime or nighttime). To asses the wind mixing impact and eliminate the diurnal warming effect, separate analyses were performed for matchup pairs with wind speeds higher than 6 m s^{-1} (daytime) and 2 m s^{-1} (nighttime), following Donlon et al (2002).

Secondly, all residuals are weighted averaged over a 7-day period to single out possible temporal/seasonal variability. The 7-day period was chosen to balance the temporal variability and

the number of residuals available for averaging. There were on average 30 residuals from the drifter MDB and 15 residuals from the platform MDB per 7-day period. Four different time-series analyses (drifters-daytime, drifters-nighttime, platform-daytime, platform-nighttime) were performed for each satellite SST product, but only drifter results will be elaborated in more detail. Filtering residuals for higher wind speeds significantly decreases the number of available residuals, preventing a time-series analysis.

4.1 Overall statistics

Overall statistics for each MDB and time period is presented separately for all wind speeds (Table 2a) and for higher wind speeds (Table 2b). For all wind speeds, positive bias values dominate the daytime results, while both positive and negative bias values appear for nighttime, depending on the algorithm and sensor. Daytime local AVHRR-derived SSTs show similar higher positive biases in all comparisons with in situ data (between 0.43 K to 0.52 K), whereas MODIS-derived SSTs exhibit smaller bias values both for the drifter and platform MDBs (between +0.10 K and +0.32 K). SDs for all daytime MDBs are between 0.5 K and 0.7 K, with only Pathfinder exhibiting a lower SD (0.36 K). Nighttime results exhibit different characteristics: local AVHRR MCTriple products exhibit negative biases (between -0.33 K and -0.18 K), while NLSST nighttime products show a bias between -0.11 and 0.12 K; the MODIS products, after skin-to-sub-skin correction is performed, exhibit absolute biases within ±0.15 K (except the Aqua-drifter MDB, which shows a higher absolute bias of -0.23 K). Pathfinder MDB biases are different for drifter- and platform-based measurements, with values of -0.06 K and 0.21 K respectively. For all MDBs, the nighttime SDs span the 0.3 K to 0.6 K range, with local AVHRR and MODIS products, employing SWIR channels by night, staying close to 0.3 K; only the Aqua/MODSST4, when compared to drifter data, generated an SD of 0.4 K. It is informative to compare the SWIR-based nighttime results for fixed (MCTriple) and variable (MODSST4) sets of coefficients. Although the overall bias of the MODSST4 algorithm is closer to zero, its overall SD is higher (by up to 0.1 K, depending on the satellite and in situ dataset) than the one for the MCTriple product (Table 2a). This demonstrates that the use of a variable set of coefficients in an algorithm which utilises SWIR channels can lead to a degradation of results.

For higher wind speeds (stratification destroyed), there is a drop of daytime bias in all SST products, while the nighttime biases perhaps predictably remain similar (Table 2b). Drifter-based daytime bias decreases are more pronounced for afternoon satellites (better developed prior stratification) and for algorithms with a fixed set of coefficients (0.3 K and 0.2 K for NOAA16/NLSST and Aqua/MODSST respectively). The mid-morning satellite decrease is lower

(about 0.15 K). For platform measurements there is practically no change in bias for mid-morning satellite-based (NOAA17, Terra) products, whereas the decrease for afternoon satellites is similar to drifter measurements.

Intercomparison of Pathfinder-, NOAA17/NLSST- and Terra/MODSST-derived SSTs is instructive due to the similarities in the algorithms and overpass times. During both the daytime and nighttime, all three products exhibit similar biases (within 0.2 K) but different SDs. During the daytime, the Pathfinder algorithm has the smallest SD, while during the nighttime it has the highest. The nighttime difference between the Pathfinder and Terra/MODSST estimates can be ascribed to different reference temperatures: Reynolds OISSTv2 for Pathfinder and MODSST4 for MODSST. The use of MODSST4 as a nighttime reference temperature provides better precision and therefore a lower SD compared to the Reynolds OISSTv2. Although the same reference temperature is used in both the MODSST and Pathfinder algorithms, the latter outperforms the former during the daytime for both in situ datasets. Compared to the implicit accommodation of the skin-to-bulk relation in AVHRR-based coefficients, the simple MODIS skin-to-bulk correction that we applied appears inadequate. Another difference is coarser Pathfinder resolution, which effectively smoothes out the SST estimate and consequently lowers its SD. It has been demonstrated that increasing the area around the central pixel to 3x3 pixels correspondingly lowers the SD by up to 0.1K, without significantly changing the bias. Further enlargement of the area around the central pixel does not improve the SD, but does increase the absolute bias (Tomazic, 2006).

The number of available residuals used in calculating statistics deserves comment. One readily notes certain intra-sensor similarities and inter-sensor differences. For instance, local NOAA16- and NOAA17-based MDBs have a similar number of matchups suggesting consistency, but not necessarily correctness, in cloudmasking. More conservative local AVHRR cloudmasking (implementing additional CH4-CH5 criteria) may result in false rejection, whereas a lack of additional channels is conducive to false acceptance. Compared to the AVHRR, the MODIS-based MDBs have a higher number of available matchups (20% to 40%), partly because of their more sophisticated cloudmasking, which based on extra channels suitable for cloud detection, reduces both false detections and false acceptances. Pathfinder has the smallest number of matchups (30% to 50% less than MODIS-based MDBs), which is most likely due to the lower spatial resolution (a higher possibility of false cloud contamination) and due to the fact that this dataset is already temporally sampled to only two results per 24-hour day (daytime and nighttime), eliminating possible multiple daily satellite observations of the same point. Higher wind-speed filtering also reduces the number of matchups by as much as 80% in the daytime.

4.2 Time-series analysis

In order to better understand the overall statistics, it is important to look at the residuals time-series (Figure 2a). The AVHRR-based datasets analysis shows a high seasonal change for daytime values with lower absolute biases during the first two quarters and pronounced higher positive biases (up to 1 K) during the third quarter of the year. A higher bias is the consequence of combined inadequate marine (diurnal warming) and atmospheric (water vapour) correction. The operational coefficients used in the local NOAA16 and NOAA17 SST estimates are derived from regression with drifting and moored buoy data (Li et al, 2000, May et al, 1998). Buoy temperature sensors are located at a depth of around 1 metre (bulk), whereas satellite sensors measure infrared radiation from the first 10 μm of the sea (skin). During the summer season, in low wind conditions there is a high temperature stratification in the initial metres which can lead to differences of several Kelvins between the skin and bulk temperature (Minnett, 2003). This stratification breaks at higher wind speeds (above 6 m s^{-1}) (Donlon et al, 2002) when a quasi homogenous layer is formed. Since operational coefficients are derived from different in situ data (drifting and moored buoys - NDBC, TOGA-TAO, AOML, MEDS, etc) mainly deployed in regions characterised by higher wind speed regimes (more than 6 m s^{-1}), their application to the Adriatic is not straightforward. On a global scale, the wind speed distribution from the F-13 SSM/I instrument for the period between 1995 and 1999 gives an average wind speed of 8.3 m s^{-1}, with approximately 30% of all wind vectors having a magnitude of less than 6 m s^{-1} and only 3% less than 2 m s^{-1} (Donlon et al, 2002). For the Adriatic region, wind speed distribution derived at drifter positions from the LAMI model for the year 2003 shows an average speed of 4.3 m s^{-1}, with more than 70% of all wind vectors having a magnitude of less than 6 m s^{-1}, and 25% of them having a magnitude of less than 2 m s^{-1}. Partial validation of the LAMI wind magnitude and direction by Signell et al (2005) suggests an eight percent model underestimation of the wind magnitude implicit in the operational SST regression, though even after applying this correction the Adriatic wind speed is appreciably smaller than the ocean wind speed. A COGOW subset is used to further examine and confirm this wind-speed discrepancy. As the majority of drifter- and platform-derived data was collected in the northern half of the Adriatic (Figure 1), the COGOW subset was taken for that area. The resulting climatology for the 2000-2004 period shows that the average wind magnitude for the northern Adriatic is 5.7 m s^{-1}, with 60% of the data having a magnitude below 6 m s^{-1}, in accordance with the corrected LAMI result. Another insightful result is the monthly distribution of less than 6 m s^{-1} wind speed for the northern half of the Adriatic (Figure 3). In the Adriatic and Mediterranean, there is again a high seasonal change, with lower winds during the third quarter of the year and higher ones during the first and

fourth quarters. The northern part of the Adriatic Sea has clearly the highest percentage of winds below 6 m s^{-1} (about 80% during the third quarter of the year), which is visible in both the COGOW and LAMI data for 2003. A similar analysis from the COGOW database, but applied to a region of TOGA-TAO buoy data in the open ocean, shows no seasonal change, and only 20% to 30% of the data have a wind speed of less than 6 m s^{-1} (Figure 3), which is similar to the global ocean result of Donlon et al (2002). Consequently, the use of operational coefficients is likely to produce a biased estimation of bulk Adriatic SST. This is evident in the third quarter of the year for all AVHRR-based SST products with a fixed set of coefficients.

Another important factor affecting the SST retrieval is atmospheric correction, mainly influenced by atmospheric water vapour. Seasonal Adriatic tcwv variability (Figure 4), derived both from Aqua/MODIS and ERA40, showed increased values in the summer months, but a lack of knowledge of the exact atmospheric a priori state for which the operational coefficients were derived precluded a comparison with global tcwv variability. Additionally, pronounced heating in the second and especially in the third quarter of the year, combined with the seasonally increased tcwv values, gives a masked SST signal that deserves further, separate analysis. Therefore, we can focus only on the end of the first quarter (March), when there were enough matchup pairs and no pronounced heating, making the atmospheric interference more visible. In this period, there were two tcwv oscillations that left their mark on all LWIR-based algorithms and satellite platforms both in the daytime and nighttime residuals (Figure 2a and Figure 2c). This dependence calls for further verification and research promising possible future improvements.

Nighttime analysis of the SST MDBs shows a better precision than the accuracy of products that use SWIR channels (MCTriple and MODSST4 - Figure 2b). A relatively high but negative bias (different for AVHRR and MODIS sensors) is almost constant throughout the year (Figure 2b), creating a small SD (from 0.3 K to 0.4 K) that varies with the MDB. The nighttime algorithms that use only the LWIR channels (Figure 2c) show a seasonal change, probably affected by an increased amount of tcwv (Figure 4) not adequately accounted for derivation of the operational coefficients. Although the overall bias in Pathfinder is relatively small (-0.06 K for drifter-based data), the time-series analysis (Figure 2b) suggests cancellation of higher positive biases during the third quarter and negative biases during the first and second quarters of the year. One should also note the uneven annual distribution of matchups that favour the third quarter of the year in calculating overall statistics. The number of matchups in the first two quarters is 10-50 per week, whereas during the third quarter there are 50-100 matchups per week.

Another piece of information which can be derived from the time-series for each MDB is the difference between daytime and nighttime residuals. Such a difference provides a new insight into the differences between the algorithms that use the same (MODIS, Pathfinder) and those that use a separate (local AVHRR) set of coefficients for daytime and nighttime, but also between those using SWIR and those employing LWIR algorithms during the nighttime. If influenced only by random physical factors and exposed to error cancellation, the residuals and their daytime-nighttime differences should be generally invariant. It is worth noting that although the absolute residuals are contaminated with matchup pair measurement discrepancies in space (vertical, horizontal) and time, all satellite products are similarly affected by these discrepancies. To eliminate the shorter period variability in the daytime-nighttime differences, a Butterworth filter with a cut-off period of two weeks was applied (Figure 5). The AVHRR-based differences are shown in Figure 5a and those based on MODIS in Figure 5b. We will first contrast the nighttime algorithms: NOAA16(NOAA17)/NLSST vs. NOAA16(NOAA17)/MCTriple, and Terra(Aqua)/MODSST vs. Terra(Aqua)/MODSST4. For the local AVHRR-based products (Figure 5a), there is a clear covariation of both algorithm solutions in the first part of the year (until late June), both for the NOAA16 and NOAA17 platforms, suggesting that the noted satellite-minus-in situ difference is not a consequence of the algorithm type. In the remaining (warmer) part of the year, the discrepancy between NLSST and MCTriple solutions (both NOAA16 and NOAA17) grows and culminates in August. The change is reflected in the pattern of covariability as well. In the first part of the year, the grouping was platform-based (e.g. the NOAA16 NLSST-NLSST curve covarying with the NOAA16 NLSST-MCTriple curve, whereas in the second it is more algorithm-based (e.g. the NOAA16 NLSST-MCTriple curve covarying with the NOAA17 NLSST-MCTriple). NLSST-MCTriple differences are greater compared to NLSST-NLSST ones because the better, constant MCTriple nighttime residuals (Figure 2b) are smaller than the erroneous NLSST ones, whereas the two NLSST-based ones offer similar, albeit erroneous, solutions. The MODIS-based residual differences (Figure 5b) exhibit very similar variability. However, contrary to the AVHRR dichotomy (NLSST-NLSST vs NLSST-MCTriple), the MODSST-MODSST and MODSST-MODSST4 residual differences are closer to each other for both Aqua and Terra mainly because the MODSST4 algorithm was used as the reference temperature for the MODSST algorithm.

It should be reiterated that the two tcwv oscillations in March (Figure 4) are even more strongly visible in the day-night differences for both AVHRR- and MODIS-based products. This provides further motivation for seeking improvements in SST retrieval.

4.3 Correlation analysis

Correlation coefficients (Table 3) between MDB pairs systematically reveal information about possible residual dependencies caused by a grouped influence of physical (atmospheric correction), technical (sensor type) and environmental factors (satellite overpass time). The higher correlations obtained between MDB pairs suggest the existence of coherent influences of the above-mentioned factors. The correlations in Table 3 are diagonally separated in two parts, the upper-right part giving the daytime correlation coefficients, and the lower-left part providing the nighttime correlations. In the daytime correlation part, the highest correlation (about 0.8) is found between the mid-morning satellites (NOAA17 and Terra, regardless of the algorithm), and between the same algorithms (NLSST or MODSST) regardless of the satellite platform. A lower daytime correlation (0.7) is obtained for the afternoon satellites with different algorithms (Aqua/MODSST vs. NOAA16/NLSST), which can possibly be ascribed to the different parameterisation of the diurnal warming influence. The correlations between Pathfinder and Terra/MODSST as well as Pathfinder and NOAA17/NLSST are about 20% higher (~0.75) than those of Pathfinder with Aqua/MODSST and with NOAA16/NLSST. Nighttime results (Table 3 lower left) resemble the daytime grouping. Higher correlations are obtained for satellites with a similar overpass time and for the same algorithm types but different satellite platforms. Correlations between the algorithms with SWIR channels (MCTriple and MODSST4) show much lower correlations (about 0.5), but nevertheless exhibit the same trend of higher correlation for similar satellites and the same type of algorithms. A lower nighttime correlation can be ascribed to the better atmospheric correction of the SWIR channel algorithms and consequently less residual influence of water vapour variability.

4.4 Local coefficients validation

The possibility of improving the local NOAA16 and NOAA17 estimated using the drifter SST data was also explored. To that end, new sets of NLSST/MCTriple coefficients were generated for each satellite by regressing the NOAA16 and NOAA17 BTs with the coincident drifter SST measurements applying the same filtering criteria. The new coefficients were then used to derive a SST for comparison with an independent shipborne and platform in situ dataset, but also for a reference self-fitting to the drifter data themselves. Applying a new set of coefficients to the same drifter dataset gives an expectedly zero bias with a lower daytime SD (~0.6 K) and a nighttime SD the same as that obtained with operational coefficients (~0.3 K) (Table 4, Table 2a). For the independent platform dataset, the bias decreases to near-zero values (except for NOAA17/MCTriple) with no change in the SD. Results for the daytime shipborne dataset exhibit a decrease in bias by 0.2 K and 0.3 K for the local NOAA16 and NOAA17 satellites respectively; the

SD remains the same and relatively high (~0.65 K) for both satellites. Analysis of individual shipborne residuals for the drifter-based algorithm (Figure 6) shows an improvement (smaller bias) in the third quarter of the year for both satellites, whereas during the first half of the year the change for NOAA16 is for the worse, and for NOAA17 there is no change. It can be argued for both platforms (NOAA16 in particular) that daily warming of the surface layer and the absence of stronger wind adversely affects the calculation of new coefficients, thereby reversing the positive effect of the atmospheric correction in the first half of the year. A similar bias improvement is obtained with another method (not presented), namely by applying the daily biases derived from the drifter-based time-series analysis to each matchup in the independent shipborne MDB for each corresponding day. This testifies to the similar effect of the two techniques in a small region, but does not help in reducing the SD.

5 Conclusions

Nine Adriatic-focused (five AVHRR-based and four MODIS-based) satellite SST products were analysed and compared with two different sets of in situ SST measurements; an additional shipborne set was used to validate the new SST coefficients. Four products were derived using locally received AVHRR telemetry and applying operational SST coefficients, whereas the other five were processed elsewhere. Five SST products were derived using LWIR channels and four were based on SWIR channels employing either fixed or variable sets of coefficients. The performance of each satellite SST product was analysed in two ways: in terms of overall statistics and as a time-series of seven-day windowed weighted moving averages. Results show an overall better performance for MODIS-based SST products, with a better accuracy (smaller bias) and similar precision (SD) compared to AVHRR-based SST products when comparing all available platforms, in situ datasets and day/night retrievals. Focusing on the daytime only, Aqua/MODSST has the lowest bias (0.1 K to 0.3 K), while Pathfinder has the lowest SD (0.3 K to 0.5 K - depending on the in situ dataset). During the nighttime, algorithms based on SWIR channels outperform LWIR channel-based algorithms with better results for MCTriple products compared to MODSST4. Although the MCTriple bias is negative (close to -0.3 K), the SD is exceptionally small (around 0.3 K) providing AATSR-like precision (reported in O'Carroll et al, 2006), and with the proper bias correction, this product is recommended for future analysis. Negative nighttime biases, common to the majority of AVHRR-based SST solutions, appear to have a common regional origin, but a more conclusive explanation of their cause requires further analysis of the atmospheric effects. Analysis performed by applying seven-day-window weighted moving averaging has shown clear seasonal variability in all residual daytime series; the variation was in response to diurnal warming, annual

change in atmospheric water vapour, and the Adriatic wind regime. Obtained residual differences were found to covary with daily water vapour changes in the first half of 2003, when there was no intensive warming of the surface. Inspection and cross-comparison of wind data from several sources confirmed a suspected significant difference between the open ocean (implicit in operational coefficients) and the Adriatic wind regime. By eliminating low wind matchup pairs (for the daytime, those with less than 6 m s^{-1}), the overall SD remains the same and biases decrease by up to 0.3 K, but are still mainly positive. The remaining bias could be ascribed to the overall atmospheric first state error. In an additional validation exercise, a new set of coefficients derived from the drifter data were used to generate SST estimates which were then compared to an independent set of shipborne and platform measurements. A decrease of absolute bias to near-zero values for platform-based validations, and for shipborne validations to 0.2 K to 0.3 K, suggests that local coefficients on average better estimate SST in the Adriatic Sea by incorporating both the influence of Adriatic-specific atmospheric correction and the joint effects of diurnal warming and a low wind regime. However, daytime SD remains the same, and relatively high for both comparisons calling for further separate consideration of the problem. The noted similar effect of the water vapour on all SST products provides a strong impetus for seeking further improvements on a regional, Adriatic scale, bearing in mind unavoidable systematic errors.

Acknowledgements

This work was supported by the Croatian Ministry of Science, Education and Sport under contract 098-0982705-2707. The DOLCEVITA drifter project was supported by the United States Office of Naval Research. We thank Dr. J. Chiggiato for the provided LAMI wind data and anonymous reviewers for helpful and useful suggestions for improving this article.

Appendix A

AAPP	ATOVS and AVHRR Pre-Processing Package
AATSR	Advanced Along Track Scanning Radiometer
ADRICOSM	Adriatic Sea Integrated Coastal Areas and River Basin Management System
ANA-3	Automatic Navigation Adjustment
AOML	Atlantic Oceanographic and Meteorological Laboratory
ATOVS	Advanced TOVS
ARGOS	Advanced Research and Global Observation Satellite
AVHRR	Advanced Very High Resolution Radiometer
BT	Brightness Temperature
CMS	Centre de Météorologie Spatiale

CODE	Coastal Ocean Dynamics Experiment
COGOW	Climatology of Global Ocean Winds
CTD	Conductivity, Temperature, Depth
DOLCEVITA	Dynamics of Localised Currents and Eddy Variability in the Adriatic
ECMWF	European Centre for Medium-Range Weather Forecasts
ERA-40	ECMWF Re-Analysis for 40 years
GHRSST-PP	GODAE High-Resolution Sea Surface Temperature Pilot Project
GODAE	Global Ocean Data Assimilation Experiment
GPS	Global Positioning System
GSFC	Goddard Space Flight Center
HRPT	High Resolution Picture Transmission
IR	Infra Red
L1B	Level 1B
L2	Level 2
LAMI	Local Area Model Italy
LWIR	Long Wave Infra Red
M-AERI	Marine-Atmosphere Emitted Radiance Interferometer
MCSST	Multi Channel Split SST Algorithm
MCTriple	Multi Channel Triple SST Algorithm
MDB	Matchup Database
MEDS	Marine Environmental Data Service
Metop-A	(Europe's first) Meteorological Operational Polar-orbiting Satellite
MODIS	Moderate-Resolution Imaging Spectrometer
MODSST	MODIS SST algorithm based on LWIR channels
MODSST4	MODIS SST algorithm based on SWIR channels
NASA	National Aeronautics and Space Administration
NDBC	National Data Buoy Center
NESDIS	National Environmental Satellite, Data, and Information Service
NLSST	Non-Linear SST algorithm
NOAA	National Oceanic and Atmospheric Administration
NWP	Numerical Weather Prediction
OBPG	Ocean Biology Processing Group
OE	Optimal Estimation
OGS	Osservatorio Geofisico Sperimentale
OISSTv2	Optimum Interpolation Sea Surface Temperature 2nd version
PO.DAAC	Physical Oceanography Distributed Active Archive Center
RBI	Rudjer Boskovic Institute
RSMAS	Rosenstiel School of Marine and Atmospheric Science
SAF	Satellite Application Facility
SD	Standard Deviation
SSES	Sensor Specific Error Statistics
SSM/I	Special Sensor Microwave Imager
SST	Sea Surface Temperature
SWIR	Short Wave Infra Red
tcwv	Total Column Water Vapour
TIROS	Television Infrared Observation Satellite
TOGA-TAO	Tropical Ocean-Global Atmosphere - Tropical Atmosphere Ocean
TOVS	TIROS Operational Vertical Sounder
UTC	Universal Time Co-ordinated
XBT	Expendable Bathythermograph

References

ADRICOSM Adriatic Sea Integrated Coastal Areas and River Basin Management System Pilot Project (ADRICOSM) 2001-2004, http://www.bo.ingv.it/adricosm

ARBELO, M., HERNANDEZ-LEAL, P., DIAZ, J.P., EXPOSITO, F.J., and HERRERA, F., 2000, Efficiency of a global algorithm for retrieving SST from satellite data in a subtropical region. *Advances in Space Research*, **25** [5], pp. 1041-1044.

ATKINSON, N.C. and DOHERY, A.M., 2005, AAPP status report and review of developments for NOAA-N and METOP. *Proc.ITSC XIV, 25-31 May 2005.*

BROWN, O.B. and MINNETT, P.J., 1999, MODIS Infrared Sea Surface Temperature Algorithm Theoretical Basis Document, Ver 2.0, http://modis.gsfc.nasa.gov/data/atbd/atbd_mod25.pdf

BRUNEL, P. and MARSOUIN, A., 2002, ANA-3 user's manual. *Météo-France/DP/CMS/R/D. 45 pp.*

CAO, C. and HEIDINGER, A., 2002, Inter-comparison of the long-wave infrared channels of MODIS and AVHRR/NOAA-16 using simultaneous nadir observations at orbit intersections. *Proceedings of SPIE*, **4814**, pp. 306-316.

CASEY, K., 2007, 4 km Pathfinder Version 5.0 User Guide, http://www.nodc.noaa.gov/SatelliteData/pathfinder4km/PFV50_UserGuide.pdf

CASTRO, S.L., WICK, G.A., JACKSON, D.L. and EMERY, W.J., 2008, Error characterization of infrared and microwave satellite sea surface temperature products for merging and analysis. *Journal of Geophysical Research*. **113**, C02010, doi: 10.1029/2006JC003829, pp. 1-17

DASH, P., IGNATOV, A., SAPPER, J., KIHAI, Y., FROLOV, A. and DE ALWIS, D., 2007, Development of a global QC/QA processor for operational NOAA 16-18 and METOP AVHRR SST products, *Proceedings of the 2007 EUMETSAT Meteorological Satellite Conference*, P.**50.**

D'ORTENZIO, F., MARULLO, S., and SANTOLERI, R., 2000, Validation of AVHRR pathfinder SST's over the Mediterranean Sea. *Geophysical Research Letters*, **27**, pp. 241-244.

DONLON, C. J., MINNETT, P., GENTEMANN, C., NIGHTINGALE, T.J., BARTON, I. J., WARD, B. and MURRAY, M. J., 2002, Toward improved validation of satellite sea surface skin temperature measurements for climate research. *Journal of Climate* **15**[4], pp. 353-369.

DONLON, C., ROBINSON, I., CASEY, K.S., VAZQUEZ-CUERVO, J., ARMSTRONG, E., ARINO O., GENTEMANN C., MAY D., LEBORGNE P., PIOLLÉ, J., BARTON, I., BEGGS, H., POULTER, D.J.S., MERCHANT, C.J., BINGHAM, A., HEINZ, S., HARRIS, A., WICK, G., EMERY, B., MINNETT, P., EVANS, R., LLEWELLYN-JONES, D., MUTLOW, C., REYNOLDS, R.W., KAWAMURA, H. and RAYNER, N., 2007, The Global Ocean Data Assimilation Experiment High-resolution Sea Surface Temperature Pilot Project. *Bulletin of the American Meteorological Society*, **88** [7], pp. 1197–1213.

EUGENIO, F., MARCELLO, J., HERNANDEZ-GUERRA, A. and ROVARIS, E., 2005, Regional optimization of an atmospheric correction algorithm for the retrieval of sea surface temperature from the Canary Islands-Azores-Gibraltar area using NOAA/AVHRR data. *International Journal of Remote Sensing,* **26**[9], pp. 1799-1814.

FELDMAN, G.C. and MCCLAIN, C.R., Ocean Color Web, MODIS Aqua and Terra SST Reprocessing V5.3 and V5.6, NASA Goddard Space Flight Center. Eds. Kuring, N., Bailey, S.W. 2007, http://oceancolor.gsfc.nasa.gov/

GOODRUM, G., KIDWELL, B.K. and WINSTON, W., 2000, NOAA KLM users's guide with NOAA-N, -N' supplement. US Department of Commerce, NOAA/NESDIS. http://www2.ncdc.noaa.gov/docs/klm/index.html

KEARNS, E.J., HANAFIN, J.A., EVANS, R.H., MINNETT, P.J. and BROWN, O.B., 2000, An independent assessment of Pathfinder AVHRR sea surface temperature accuracy using the Marine Atmosphere Emitted Radiance Interferometer (MAERI). *Bulletin of the American Meteorological Society,* **81** (7), pp. 1525-1536.

KILPATRICK, K.A., PODESTA, G. P. and EVANS, R.H., 2001, Overview of the NOAA/NASA advanced very high resolution radiometer Pathfinder algorithm for sea surface temperature and associated matchup database. *Journal of Geophysical Research,* **106**, pp. 9179-9198.

KUMAR, A., MINNET, P.J., PODESTA, G., EVANS, R.H. AND KILPATRICK, K.A., 2000, Analysis of Pathfinder SST algorithm for global and regional conditions. *The Proceedings of the Indian Academy of Sciences: Earth and Planetary Sciences*, **109**, pp. 395-405.

LEITZ, J.M., 1999, Ionian Sea surface temperature: satellite and drifter observations, May to October, 1995. *M. S. Thesis, Naval Postgraduate School, Monteray, California.* 89 pp.

LI, X., PICHEL, W., MATURI, E., CLEMENTE-COLON, P. and SAPPER, J., 2000, Deriving the operational nonlinear multichannel sea surface temperature algorithm coefficients for NOAA-15 AVHRR/3. *International Journal of Remote Sensing,* **22**[4], pp. 699-704.

MAY, D.A, PARMATER, M.M., OLSZEWSKI, D.S. and MCKENZIE, B.D., 1998, Operational processing of satellite sea surface temperature retrievals at the Naval Oceanographic Office. *Bulletin of the American* Meteorological *Society,* **79**[3], pp. 397-407.

MERCHANT, C.J., HORROCKS, L.A., EYRE, J.R. and O'CARROLL, A.G., 2006, Retrievals of sea surface temperature from infrared imagery: origin and form of systematic errors. *Q.J.R. Meterol. Soc*., **132**, pp. 1205-1223.

MERCHANT, C.J., LE BORGNE, P., MARSOUN, A. and ROQUET, H., 2008, Optimal estimation of sea surface temperature from split-window observation. *Remote Sensing of Environment*, **112**, pp. 2469-2484.

MINNETT, P.J., 2003, Radiometric measurements of the sea-surface skin temperature: the competing roles of the diurnal thermocline and the cool skin. *International Journal of Remote Sensing,* **24**[24], pp. 5033-5047.

MINNETT, P.J., BROWN, O.B., EVANS, R.H., KEY, E.L., KEARNS, E.J., KILPATRICK, K.A., KUMAR, A., MAILLET, K.A. and SZCZODRAK, G., 2004, Sea-surface temperature measurements from the Moderate-Resolution Imaging Spectrometer (MODIS) on Aqua and Terra. *Geoscience and Remote Sensing Symposium, 2004. IGARSS '04. Proceedings. 2004 IEEE Internationa*l, **7**, pp. 4576-4579.

NOTARSTEFANO, G., MAURI, E. and POULAIN, P.-M., 2006, Near-surface thermal structure and surface diurnal warming in the Adriatic Sea using satellite and drifter data. *Remote Sensing of Environment*, **101** [2], pp. 194-211.

O'CARROLL, A.G., WATTS, J.G., HORROCKS, L.A., SAUNDERS, R.W. and RAYNER, N.A., 2006. Validation of the AATSR Meteo Product Sea Surface Temperature. *Journal of Atmospheric and Oceanic Technology*, **23** [5], pp. 711-726.

POULAIN, P.-M., 2001, Adriatic Sea surface circulation as derived from drifter data between 1990 and 1999. *Journal of Marine Systems*, **29**, pp. 3-32.

RISIEN, C.M. and CHELTON, D.B., 2006, A satellite-derived climatology of global ocean winds. *Remote Sensing of Environment*, **105**, pp. 221-236.

SAUNDERS, R.W. and KRIEBEL, T.K., 1988, An improved method for detecting clear sky and cloudy radiances from AVHRR data. *International Journal of Remote Sensing*, **9**, pp. 123-150.

SEEMANN, S.W., BORBAS1, E.E., JUN, L., MENZEL, W.P. and GUMLEY, L.E., 2006, MODIS Atmospheric Profile Retrieval Algorithm Theoretical Basis Document, Ver 6, http://modis-atmos.gsfc.nasa.gov/_docs/MOD07:MYD07_ATBD_C005.pdf

SIGNELL, R.P., CARNIEL, S., CAVALERI, L., CHIGGIATO, J., DOYLE, J.D., PULLEN, J. and SCLAVO, M., 2005, Assessment of wind quality for oceanographic modelling in semi-enclosed basins. *Journal of Marine Systems*, **53**, pp. 217-233.

STOWE, L., Davis, P., and McClain, E.P., 1999, Scientific basis and initial evaluation of the CLAVR-1 global clear/cloud classification algorithm for the advanced very high resolution radiometer. *Journal of Atmosphere and Oceanic Technology*, **16**, pp. 656-681.

TOMAZIC, I., 2006, Validation of remotely sensed Adriatic Sea surface temperature (in Croatian). *MSc Thesis, Faculty of Sciences and Mathematics, University of Zagreb*, 170 pp.

TOMAZIC, I., KUZMIC, M., NOTARSTEFANO, G., MAURI, E., and POULAIN, P.-M., 2006, Improving the AVHRR estimates of the Adriatic Sea surface temperature. *Proceedings of the 2005 EUMETSAT Meteorological Satellite Conference*, P.**46**, pp. 499-504.

TOMAZIC, I., KUZMIC, M., NOTARSTEFANO, G., MAURI, E., and POULAIN, P.-M., 2007, Sensor specific error statistics: a case study of the AVHRR-derived Adriatic SST. *Proceedings of the 2007 EUMETSAT Meteorological Satellite Conference*, P.**50**.

TOMAZIC, I. and KUZMIC, M., 2009, ERA-40-aided assessment of the atmospheric influence on satellite retrieval of Adriatic Sea surface temperature. *Meteorology and Atmospheric Physics*, **104** (1-2), doi:10.1007/s00703-008-0015-2, pp. 37-51.

UPPALA, S.M., 45 Co-authors, 2005, The ERA-40 re-analysis. *Quarterly Journal of the Royal Meteorological Society,* **131**, pp. 2961–3012.

URSELLA, L., BARBANTI, R. and POULAIN, P.M.. 2004, DOLCEVITA drifter program: Rapporto tecnicio finale. *Tech.* Report. *77/2004/OGA/30, OGS, Trieste, Italy*. 31. pp

ZHANG, H.M., REYNOLDS, R.W. and SMITH, M., 2004, Bias characteristics in the AVHRR sea surface temperature. *Geophysical Research Letters*, **31,** L01307, pp. 1-4.

Table 1. SST algorithms used in the comparison of different sensors and products. T_{sfc} is an a priori estimate of the surface temperature in degrees Celsius, Θ is the satellite zenith angle, a_i are coefficients, T_λ is the brightness temperature of the sensor channel where λ (3.7, 3.9, 4.0, 11 and 12 μm) denotes the channel wavelength. The NLSST, Pathfinder and MODSST algorithms have the same form but different coefficients and a different estimated surface temperature. The NLSST algorithm uses the MCSST estimate, Pathfinder uses Reynolds OISSTv2 and MODSST uses Reynolds OISSTv2 for daytime and MODSST4 for nighttime SST estimates. The MCTriple algorithm is similar to the MODSST4 algorithm with the difference being that the MCTriple combines all three available AVHRR IR channels, whereas MODSST4 only uses channels in the short infrared region.

Name	Day/Night	Algorithm	Tsfc
NLSST	D	$a_1T_{11} + a_2T_{sfc}(T_{11}-T_{12}) + a_3(T_{11}-T_{12})(\sec\Theta-1)+a_4$	MCSST
MCTriple	N	$a_1T_{11}+a_2T_{3.7}+a_3T_{12}+a_4(T_{3.7}-T_{12})(\sec(\Theta)-1) +a_5(\sec\Theta-1)+a_6$	-
Pathfinder	D/N	$a_1T_{11} + a_2T_{sfc}(T_{11}-T_{12}) + a_3(T_{11}-T_{12})(\sec\Theta-1)+a_4$	Reynolds OISSTv2
MODSST	D/N	$a_1T_{11} + a_2T_{sfc}(T_{11}-T_{12}) + a_3(T_{11}-T_{12})(\sec\Theta-1)+a_4$	Reynolds/MODSST4
MODSST4	N	$A_1T_{3.9} + a_2(T_{3.9}-T_{4.0}) + a_3(\sec\Theta-1)+a_4$	-

Table 2. Statistics of matchup pairs for each satellite product and in situ database for the specified periods a) independent of the wind speed, and b) for daytime wind speeds higher than 6 m s^{-1} and nighttime wind speeds higher than 2 m s^{-1}. 'Bias' represents the average value of residuals, 'SD' is the corresponding standard deviation and 'N' is the number of residuals used in calculating the statistics. The overall statistics for Reynolds OISSTv2 (used in the Pathfinder product as the reference SST) were added as a reference.

a)

Satellite/ algorithm	DAY						NIGHT					
	Drifters			Platform			Drifters			Platform		
	Bias/K	SD/K	N	Bias/K	SD/K	N	Bias/K	SD/K	N	Bias/K	SD/K	N
NOAA16 NLSST	+0.43	0.72	928	+0.45	0.68	57	-0.11	0.58	895	-0.10	0.59	53
NOAA17 NLSST	+0.52	0.67	981	+0.43	0.47	65	+0.08	0.57	655	+0.12	0.55	53
NOAA16 MCTriple	-	-	-	-	-	-	-0.33	0.32	894	-0.29	0.29	53
NOAA17 MCTriple	-	-	-	-	-	-	-0.30	0.31	655	-0.18	0.27	53
Aqua MODSST	+0.10	0.61	1515	+0.28	0.63	80	-0.23	0.48	997	-0.13	0.42	67
Terra MODSST	+0.32	0.65	1332	+0.29	0.64	82	-0.05	0.42	663	+0.07	0.49	55
Aqua MODSST4	-	-	-	-	-	-	-0.08	0.41	1087	+0.02	0.33	72
Terra MODSST4	-	-	-	-	-	-	+0.02	0.31	708	+0.16	0.36	60
Pathfinder NOAA17	+0.40	0.52	511	+0.34	0.34	45	-0.02	0.67	380	+0.20	0.57	46
Reynolds OISSTv2	-0.27	0.90	510	+0.18	0.70	45	-0.59	1.05	382	+0.07	0.64	46

b)

Satellite/ algorithm	DAY						NIGHT					
	Drifters			Platform			Drifters			Platform		
	Bias/K	SD/K	N	Bias/K	SD/K	N	Bias/K	SD/K	N	Bias/K	SD/K	N
NOAA16 NLSST	+0.17	0.75	157	+0.08	0.31	12	-0.09	0.58	626	-0.08	0.59	46
NOAA17 NLSST	+0.33	0.67	199	+0.42	0.36	16	+0.12	0.55	438	+0.19	0.52	43
NOAA16 MCTriple	-	-	-	-	-	-	-0.33	0.29	625	-0.28	0.29	14
NOAA17 MCTriple	-	-	-	-	-	-	-0.30	0.29	438	-0.16	0.27	17
Aqua MODSST	-0.07	0.58	308	+0.06	0.27	13	-0.21	0.46	693	-0.10	0.37	55
Terra MODSST	+0.20	0.67	248	+0.28	0.55	19	-0.05	0.42	478	-0.01	0.41	41
Aqua MODSST4	-	-	-	-	-	-	-0.07	0.38	746	+0.04	0.30	58
Terra MODSST4	-	-	-	-	-	-	+0.01	0.30	503	+0.11	0.30	43
Pathfinder NOAA17	+0.29	0.54	122	+0.33	0.24	10	+0.09	0.57	259	+0.24	0.61	38
Reynolds	-0.28	1.03	121	+0.44	0.76	10	-0.54	0.97	261	+0.11	0.60	38

Table 3. Cross-comparison of the time-series correlation coefficients. The upper-right part of the table represents daytime correlations and the lower-left part represents nighttime correlations.

DAY/ NIGHT		NOAA16		NOAA17		AQUA		TERRA		NOAA17
		NLSST	MCTriple	NLSST	MCTriple	MODSST	MODSST4	MODSST	MODSST4	Pathfinder
NOAA16	NLSST	1.00		0.84	-	0.70	-	0.73	-	0.63
	MCTriple	0.44	1.00	-	-	-	-		-	-
NOAA17	NLSST	0.89	0.41	1.00	-	0.68	-	0.79	-	0.76
	MCTriple	0.31	0.53	0.56	1.00		-		-	-
AQUA	MODSST	0.79	0.53	0.69	0.24	1.00	-	0.81	-	0.57
	MODSST4	0.44	0.58	0.38	0.37	0.64	1.00	-	-	-
TERRA	MODSST	0.65	0.48	0.72	0.54	0.72	0.51	1.00	-	0.74
	MODSST4	0.21	0.46	0.28	0.45	0.31	0.50	0.66	1.00	-
NOAA17	Pathfinder	0.50	0.15	0.52	0.00	0.45	0.07	0.38	0.08	1.00

Table 4. Statistics of locally derived NLSST/MCTriple coefficients for available in situ datasets. Bias, SD and N as in Table 2.

Satellite	Algorithm	Coefficients	DAY/ NIGHT	Drifters			Platform			Shipborne		
				bias/K	SD/K	N	bias/K	SD/K	N	bias/K	SD/K	N
NOAA16	NLSST	Local	DAY	0.00	0.58	933	0.01	0.68	57	0.16	0.65	93
NOAA17	NLSST	Local	DAY	0.00	0.61	983	0.03	0.48	65	0.29	0.67	158
NOAA16	MCTriple	Local	NIGHT	0.00	0.32	894	0.06	0.29	53	-	-	-
NOAA17	MCTriple	Local	NIGHT	0.00	0.30	655	0.15	0.25	53	-	-	-

Figure captions

Figure 1. Position of the platform (white square) and drifters before (grey dots) and after (black dots) matching with the satellite data. The black line marks the division between the upper and lower Adriatic used in COGOW-based wind analysis.

Figure 2. Time-series of drifter-based residual statistical parameters for a) LWIR daytime, b) SWIR nighttime and c) LWIR nighttime algorithms.

Figure 3. Percentage time-series of wind with less than 6 m s^{-1} magnitude. Wind data are derived from QuikSCAT COGOW climatology (Adriatic, Mediterranean, TOGA-TAO) and from the LAMI model (at the location of the matchups) for the year 2003.

Figure 4. Northern Adriatic time-series of moving-average filtered MODIS-derived daytime (solid) and nighttime (dashed) total column water vapour in the year 2003 compared to 45 year climatological monthly values extracted from the ERA40 ECMWF data (dotted) for the whole Adriatic.

Figure 5. Time-series of differences between moving-average filtered daytime and nighttime residuals of satellite minus drifter SST for a) AVHRR and b) MODIS products. Two-week Butterworth filtering was applied to eliminate shorter periodic variability. Interpolated values required for filtering are marked with a circle. Afternoon satellites (NOAA16 and Aqua) are marked with a full line and mid-morning satellites (NOAA17 and Terra) are marked with a dashed line. The differences obtained with the LWIR nighttime algorithm are black and for the SWIR nighttime algorithm are grey.

Figure 6. Time-series of bias residuals obtained with operational (dot) and new (cross) sets of NLSST algorithm coefficients. New sets are derived from the drifter MDB and together with the operational set applied to independent shipborne-collected data, matched to NOAA16 (upper figure) and NOAA17 (lower figure) SST retrievals.

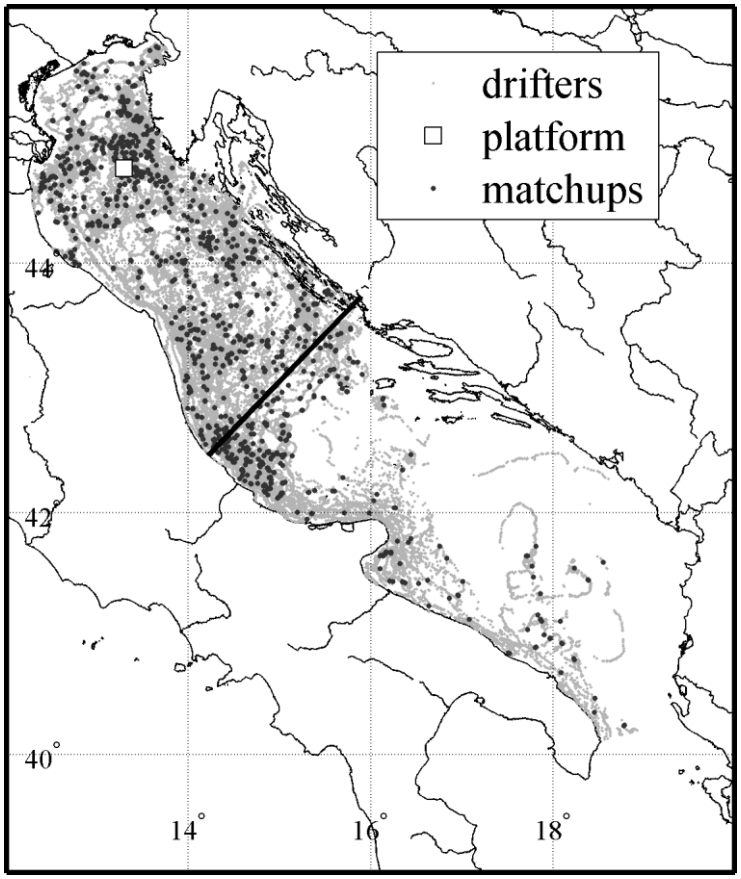

Figure 1

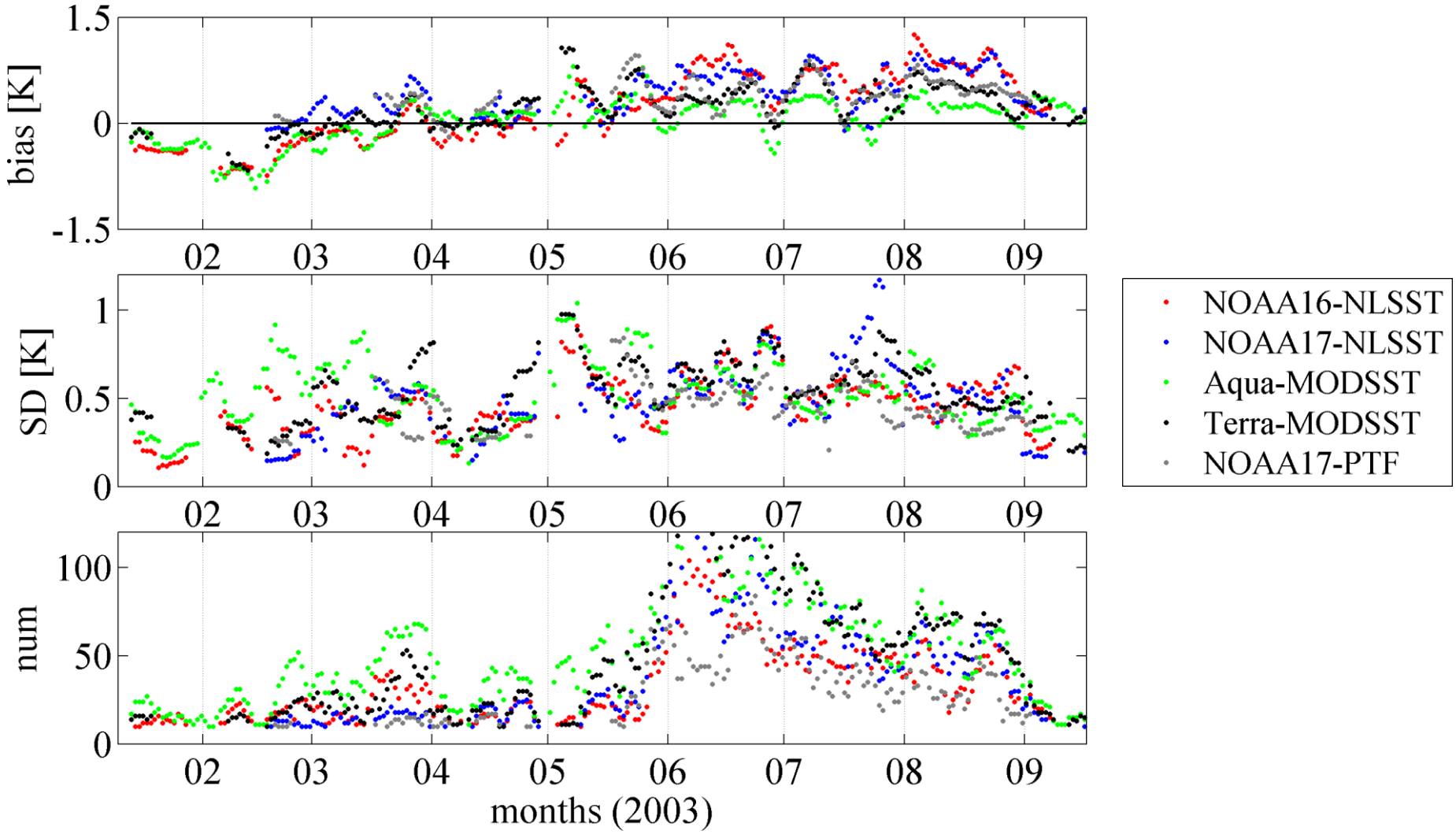
bias [K]
1.5
0
-1.5
02
03
04
05
06
07
08
09
SD [K]
1
0.5
0
num
100
50
months (2003)
NOAA16-NLSST
NOAA17-NLSST
Aqua-MODSST
Terra-MODSST
NOAA17-PTF

Figure 2a

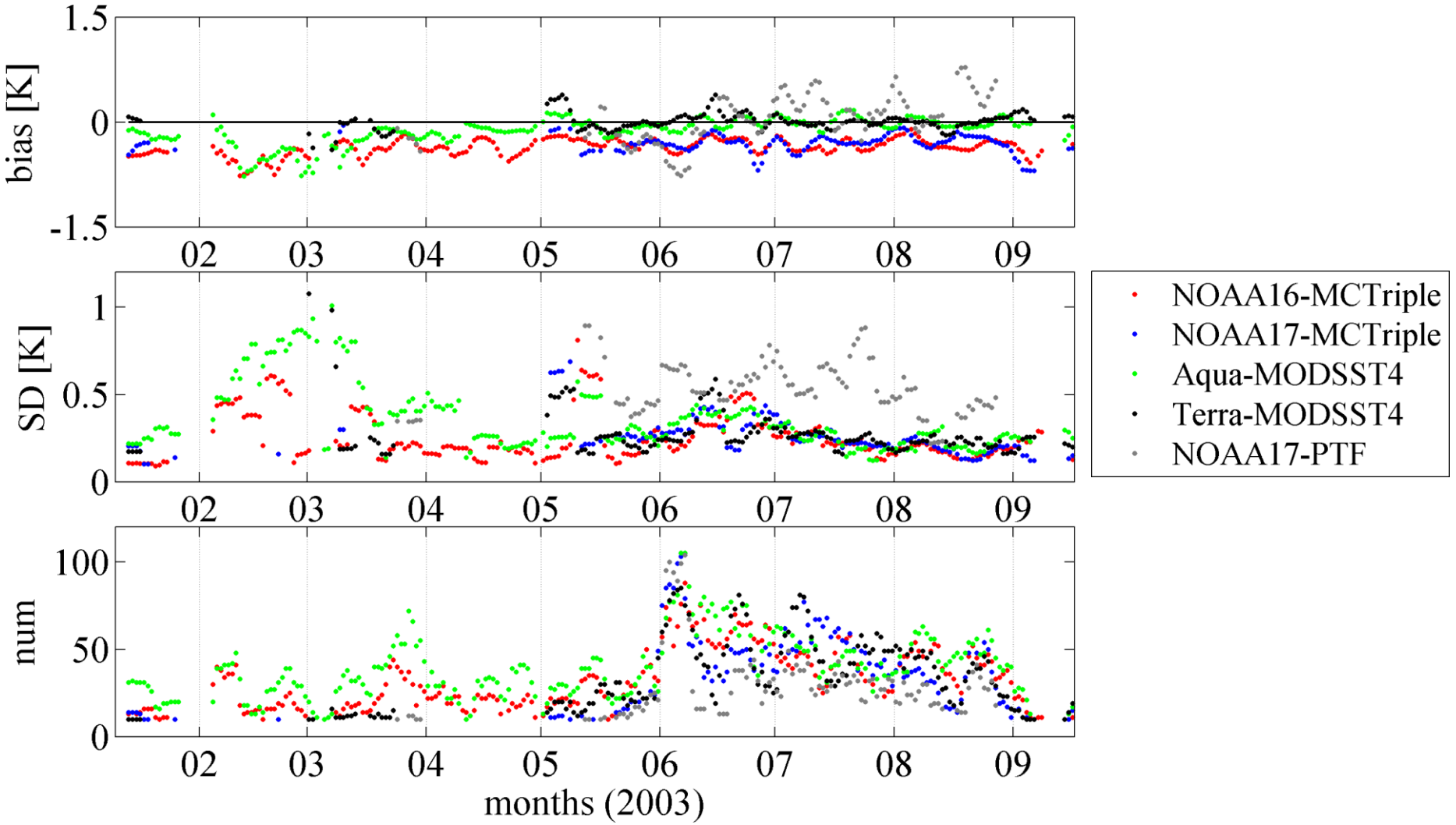
bias [K]
1.5
0
-1.5
02
03
04
05
06
07
08
09
SD [K]
1
0.5
0
num
100
50
months (2003)
NOAA16-MCTriple
NOAA17-MCTriple
Aqua-MODSST4
Terra-MODSST4
NOAA17-PTF

Figure 2b

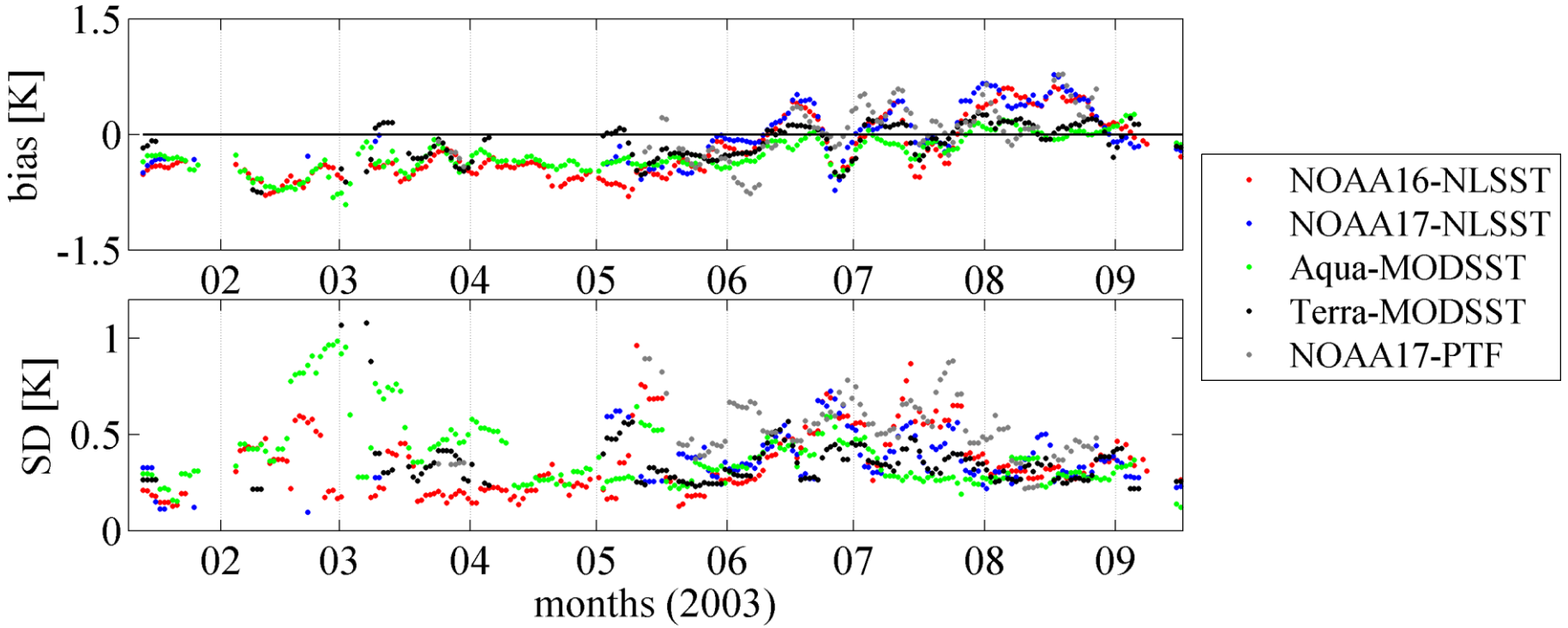
1.5
0
-1.5
bias [K]
02
03
04
05
06
07
08
09
1
0.5
0
SD [K]
months (2003)
NOAA16-NLSST
NOAA17-NLSST
Aqua-MODSST
Terra-MODSST
NOAA17-PTF

Figure 2c

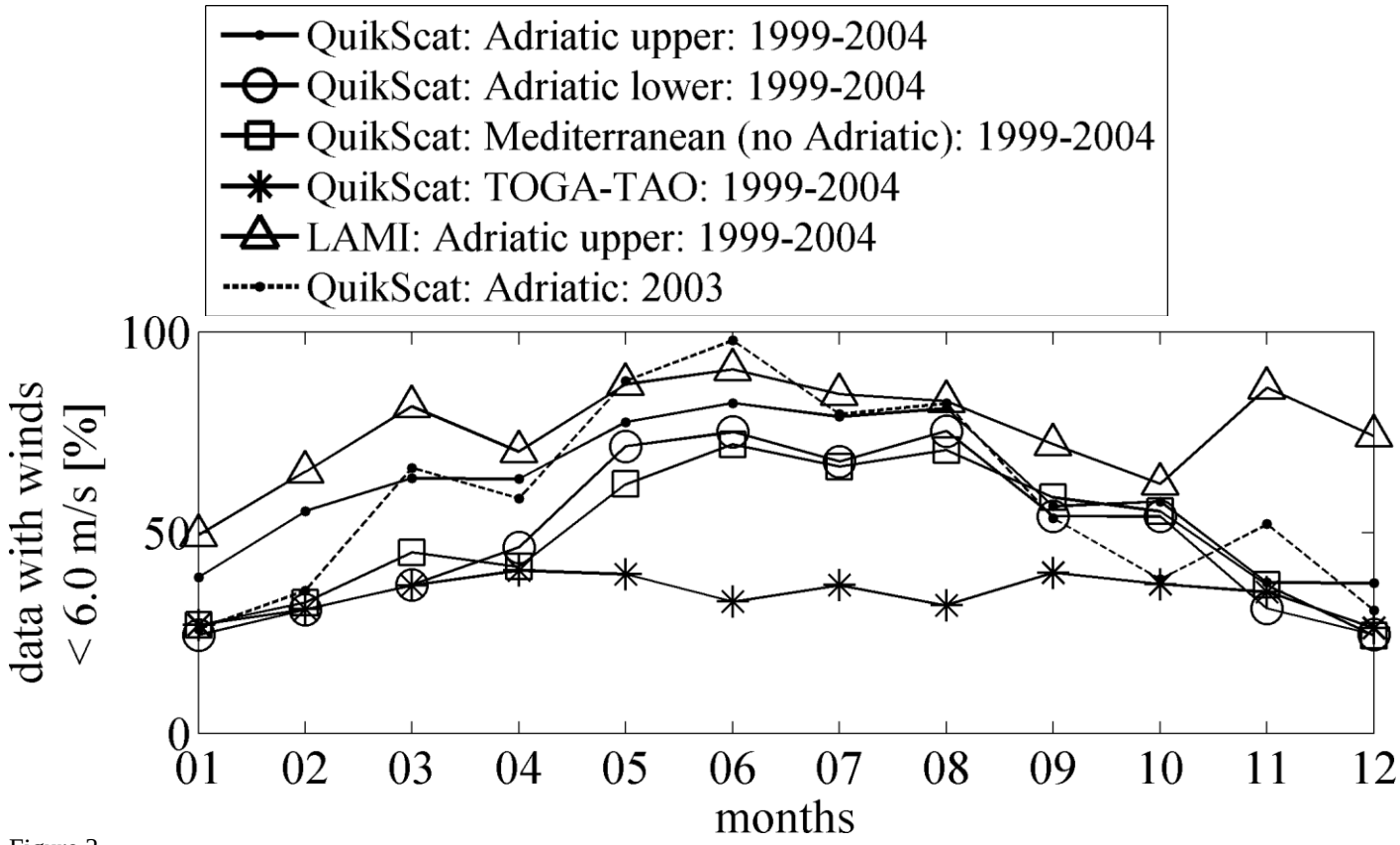
QuikScat: Adriatic upper: 1999-2004
QuikScat: Adriatic lower: 1999-2004
QuikScat: Mediterranean (no Adriatic): 1999-2004
QuikScat: TOGA-TAO: 1999-2004
LAMI: Adriatic upper: 1999-2004
QuikScat: Adriatic: 2003
data with winds < 6.0 m/s [%]
100
50
0
01
02
03
04
05
06
07
08
09
10
11
12
months

Figure 3

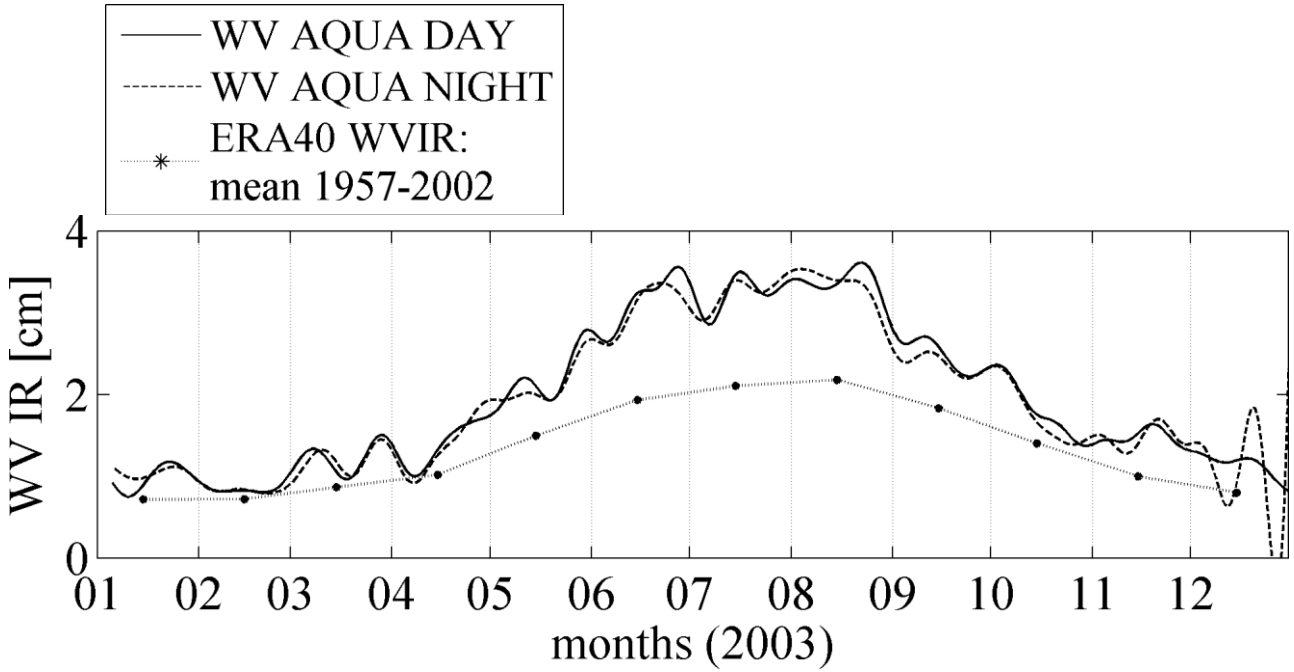
WV AQUA DAY
WV AQUA NIGHT
ERA40 WVIR:
mean 1957-2002
WV IR [cm]
0
2
4
01
02
03
04
05
06
07
08
09
10
11
12
months (2003)

Figure 4

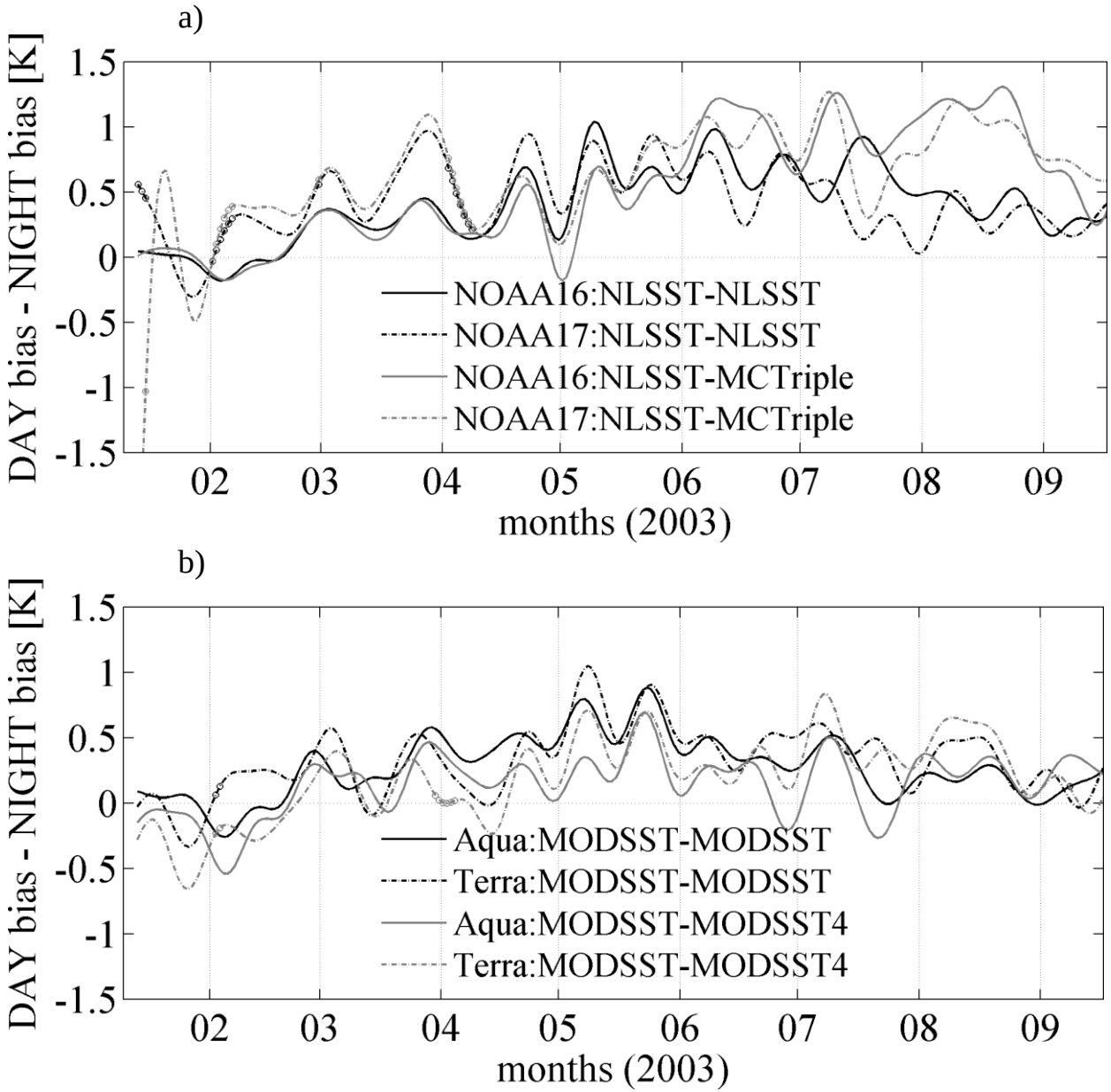
a)
DAY bias - NIGHT bias [K]
1.5
1
0.5
0
-0.5
-1
-1.5
02
03
04
05
06
07
08
09
months (2003)
NOAA16:NLSST-NLSST
NOAA17:NLSST-NLSST
NOAA16:NLSST-MCTriple
NOAA17:NLSST-MCTriple
b)
DAY bias - NIGHT bias [K]
months (2003)
Aqua:MODSST-MODSST
Terra:MODSST-MODSST
Aqua:MODSST-MODSST4
Terra:MODSST-MODSST4

Figure 5

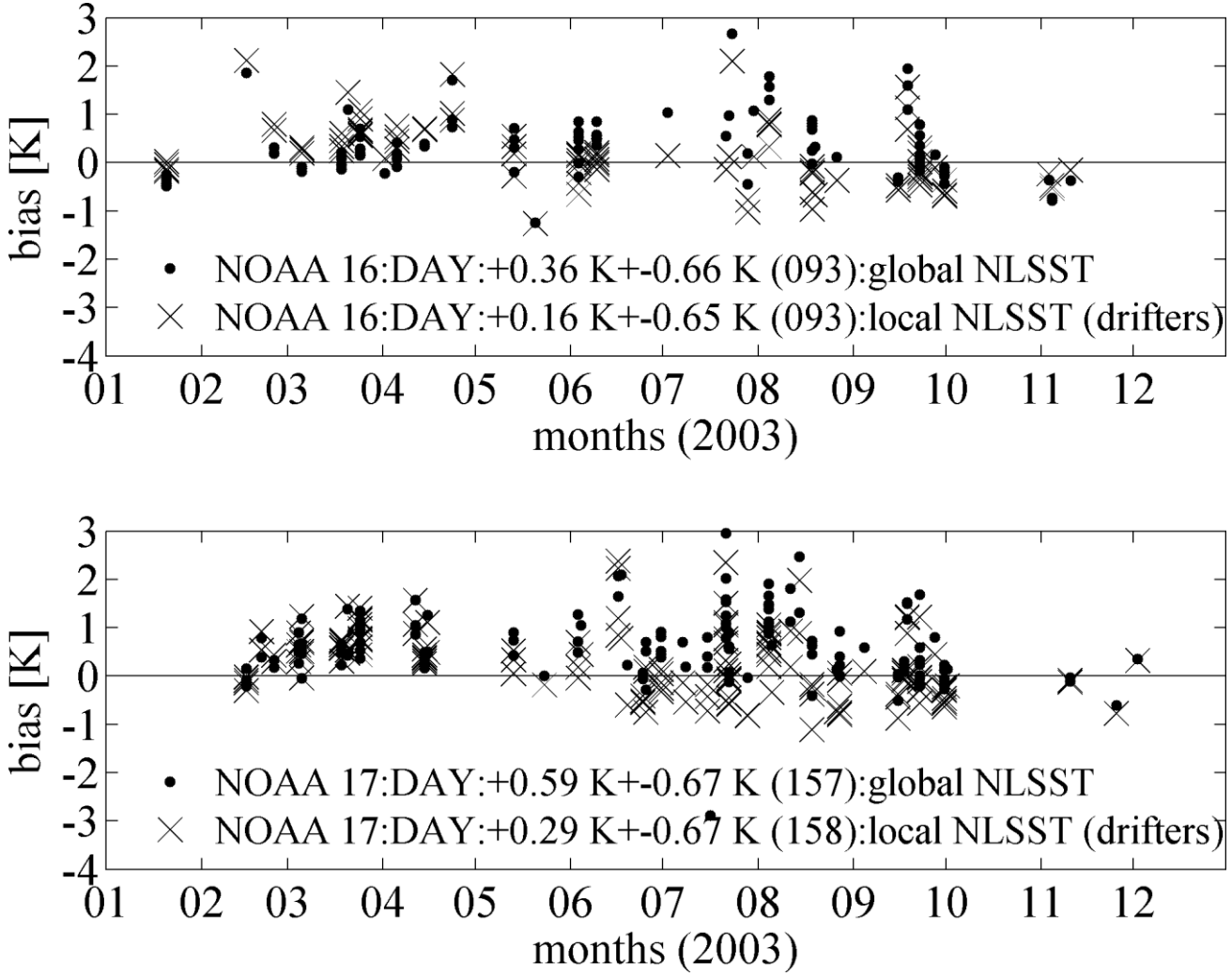
bias [K]
months (2003)
NOAA 16:DAY:+0.36 K+-0.66 K (093):global NLSST
NOAA 16:DAY:+0.16 K+-0.65 K (093):local NLSST (drifters)
NOAA 17:DAY:+0.59 K+-0.67 K (157):global NLSST
NOAA 17:DAY:+0.29 K+-0.67 K (158):local NLSST (drifters)

Figure 6